

Exotic Dark Matter Search with CDEX-10 Experiment at China Jinping Underground Laboratory

W. H. Dai,¹ L. P. Jia,¹ H. Ma,^{1,*} Q. Yue,^{1,†} K. J. Kang,¹ Y. J. Li,¹ H. P. An,² Greeshma C.,^{3,‡} J. P. Chang,⁴ Y. H. Chen,⁵ J. P. Cheng,^{1,6} Z. Deng,¹ C. H. Fang,⁷ X. P. Geng,¹ H. Gong,¹ Q. J. Guo,⁸ X. Y. Guo,⁵ L. He,⁴ S. M. He,⁵ J. W. Hu,¹ H. X. Huang,⁹ T. C. Huang,¹⁰ H. T. Jia,⁷ X. Jiang,⁷ S. Karmakar,^{3,‡} H. B. Li,^{3,‡} J. M. Li,¹ J. Li,¹ Q. Y. Li,⁷ R. M. J. Li,⁷ X. Q. Li,¹¹ Y. L. Li,¹ Y. F. Liang,¹ B. Liao,⁶ F. K. Lin,^{3,‡} S. T. Lin,⁷ S. K. Liu,⁷ Y. D. Liu,⁶ Y. Liu,⁷ Y. Y. Liu,⁶ Z. Z. Liu,¹ Y. C. Mao,⁸ Q. Y. Nie,¹ J. H. Ning,⁵ H. Pan,⁴ N. C. Qi,⁵ J. Ren,⁹ X. C. Ruan,⁹ Z. She,¹ M. K. Singh,^{3,12,‡} T. X. Sun,⁶ C. J. Tang,⁷ W. Y. Tang,¹ Y. Tian,¹ G. F. Wang,⁶ L. Wang,¹³ Q. Wang,^{1,2} Y. Wang,^{1,2} Y. X. Wang,⁸ H. T. Wong,^{3,‡} S. Y. Wu,⁵ Y. C. Wu,¹ H. Y. Xing,⁷ R. Xu,¹ Y. Xu,¹¹ T. Xue,¹ Y. L. Yan,⁷ L. T. Yang,¹ N. Yi,¹ C. X. Yu,¹¹ H. J. Yu,⁴ J. F. Yue,⁵ M. Zeng,¹ Z. Zeng,¹ B. T. Zhang,¹ F. S. Zhang,⁶ L. Zhang,⁷ Z. H. Zhang,¹ Z. Y. Zhang,¹ K. K. Zhao,⁷ M. G. Zhao,¹¹ J. F. Zhou,⁵ Z. Y. Zhou,⁹ and J. J. Zhu⁷

(CDEX Collaboration)

¹Key Laboratory of Particle and Radiation Imaging (Ministry of Education)
and Department of Engineering Physics, Tsinghua University, Beijing 100084

²Department of Physics, Tsinghua University, Beijing 100084

³Institute of Physics, Academia Sinica, Taipei 11529

⁴NUCTECH Company, Beijing 100084

⁵YaLong River Hydropower Development Company, Chengdu 610051

⁶College of Nuclear Science and Technology, Beijing Normal University, Beijing 100875

⁷College of Physics, Sichuan University, Chengdu 610065

⁸School of Physics, Peking University, Beijing 100871

⁹Department of Nuclear Physics, China Institute of Atomic Energy, Beijing 102413

¹⁰Sino-French Institute of Nuclear and Technology, Sun Yat-sen University, Zhuhai 519082

¹¹School of Physics, Nankai University, Tianjin 300071

¹²Department of Physics, Banaras Hindu University, Varanasi 221005

¹³Department of Physics, Beijing Normal University, Beijing 100875

(Dated: November 24, 2022)

A search for exotic dark matter (DM) in the sub-GeV mass range has been conducted using 205 kg-day data taken from a p-type point contact germanium detector of CDEX-10 experiment at China Jinping underground laboratory. New low-mass dark matter searching channels, neutral current fermionic DM absorption ($\chi + A \rightarrow \nu + A$) and DM-nucleus $3 \rightarrow 2$ scattering ($\chi + \chi + A \rightarrow \phi + A$), have been analyzed with an energy threshold of 160 eVee. No significant signal was found, thus new limits on the DM-nucleon interaction cross section are set for both models at sub-GeV DM mass region. A cross section limit for the fermionic DM absorption is set to be $2.5 \times 10^{-46} \text{ cm}^2$ (90% C.L.) at DM mass of 10 MeV/ c^2 . For the DM-nucleus $3 \rightarrow 2$ scattering scenario, limits are extended to DM mass of 5 MeV/ c^2 and 14 MeV/ c^2 for the massless dark photon and bound DM final state, respectively.

Key words: sub-GeV dark matter, fermionic dark matter absorption, DM-nucleus $3 \rightarrow 2$ scattering, CJPL.

Introduction- Various evidence from cosmological and astronomical observations strongly supports the existence of dark matter (DM) in our Universe [1]. The weakly interacting massive particle (WIMP) DM candidate has been searched for several decades [2-4], and the limit on the WIMP-nucleus cross section has been pushed near the neutrino floor for DM masses around the GeV scale in direct detection experiments [5-12].

The null results in WIMP search have motivated building of alternative dark matter models [13-15]. Recently, two sub-GeV light DM interaction scenarios, the neutral current fermionic DM absorption and DM-nucleus $3 \rightarrow 2$

scattering, have been proposed and searched for experimentally [16-21].

The fermionic DM (χ) may convert to a neutrino (ν) upon interaction with a target (A) via a neutral current absorption process ($\chi + A \rightarrow \nu + A$) [16,17]. The absorption generates a monoenergetic signal with an energy proportional to the DM mass in direct detection experiments. Experiments with a low energy threshold, low background, and good energy resolution can provide strong constraints on the interaction cross section. In direct detection experiments, only two searches have been performed to date. The most stringent limit at 15~125 MeV/ c^2 DM mass range is given by PandaX-4T experiment and the lowest limit on the cross section of $1.7 \times 10^{-50} \text{ cm}^2$ (90% C.L.) is placed at DM mass of 35 MeV/ c^2 [18]. The MAJORANA DEMONSTRATOR set limits on the fermionic DM absorption cross section at the

* mahao@tsinghua.edu.cn

† yueq@mail.tsinghua.edu.cn

‡ Participating as a member of TEXONO Collaboration

DM mass of 25~190 MeV/c² via the high purity germanium detector technology [19].

In recent work, another direct detection channel for sub-GeV DM via a DM-nucleus 3→2 scattering process ($\chi + \chi + A \rightarrow \phi + A$) is proposed [21]. Two DM candidates (χ) may combine into a DM composite state or dark radiation (ϕ) upon the interaction with a target (A). Similar to the fermionic DM absorption, a monoenergetic signal is generated in the three-body scattering, and the energy passed to the nucleon is related to the mass of the initial and final states of DM. The MAJORANA DEMONSTRATOR performed searches for DM-nucleus 3→2 scattering signals with 52.6 kg-year exposure data and an analysis threshold of 1 keVee [19].

In this letter, we report the search results of the neutral current fermionic DM absorption and DM-nucleus 3→2 scattering using 205 kg-day exposure data from the CDEX-10 experiment with an analysis threshold of 160 eVee.

CDEX-10 Experiment- The CDEX-10 experiment operates a 10-kg p-type point contact germanium (PPCGe) detector array to search for light DM in China Jinping Underground Laboratory (CJPL) [11,22]. The detector array consists of three triple-element PPCGe detector strings, C10-A, B, C, respectively. The detector array surrounded by a 20 cm high-purity oxygen-free copper shielding is directly immersed in a liquid nitrogen (LN) cryostat for cooling. The LN cryostat and data acquisition (DAQ) systems are placed inside a polyethylene room at CJPL-I [23]. The detailed configuration of the experimental setup can be found in [11,23].

One of the C10 detectors, C10-B1, achieved the lowest analysis threshold (160 eVee) during its data taking from February 2017 to August 2018 [11,24]. The dead layer thickness of C10-B1 is evaluated to be (0.88 ± 0.12) mm [11,12]. The dead layer results in a fiducial mass of 939 g and, accordingly, an exposure of 205 kg-day.

The data processing procedures, including energy calibration, pedestal cut, physics event selection, and bulk or surface event discrimination, were discussed in our previous works [11,25]. The dead time of the DAQ system was measured to be 5.7% by random trigger signals. Efficiencies of event trigger and event selection were derived from a ¹³⁷Cs source following the method described in our previous works [11,12]. The analysis threshold is selected to be 160 eVee, corresponding to a combined efficiency of $(5.7 \pm 1.48)\%$. The 0.16~4 keVee spectrum after all event selections and efficiency correction is used for DM analysis.

Data Analysis- A minimum χ^2 method, similar to our previous WIMP analysis [11,24,26], is used to search for the fermionic DM absorption and DM-nucleus 3→2 scattering. The χ^2 is constructed as

$$\chi^2 = \sum_i \frac{[n_i - S_i(m_\chi, \sigma_\chi) - B_i]^2}{\sigma_{stat,i}^2 + \sigma_{syst,i}^2}, \quad (1)$$

where n_i is the measured event rate in i^{th} energy bin,

$\sigma_{stat,i}$ and $\sigma_{syst,i}$ are the statistical and systematic uncertainty, respectively. The systematic uncertainty includes uncertainties in exposure, event select efficiency and bulk/surface event discrimination [11]. $S_i(m_\chi, \sigma_\chi)$ is the expected DM event rate in i^{th} energy bin at DM mass m_χ and DM-nucleus interaction cross section σ_χ . B_i is the background event rate in the i^{th} energy bin.

The background event rate (B , in counts per keVee per kg per day) of C10-B1 detector consists of a flat continuum (p_0) plus L-shell and M-shell X-ray peaks from ⁶⁸Ge ($E_L = 1.298$ keV, $E_M = 0.16$ keV), ⁶⁸Ga ($E_L = 1.194$ keV, $E_M = 0.14$ keV), ⁶⁵Zn ($E_L = 1.096$ keV), ⁵⁵Fe ($E_L = 0.764$ keV), ⁵⁴Mn ($E_L = 0.695$ keV), and ⁴⁹V ($E_L = 0.564$ keV):

$$B = p_0 + \sum_L I_L \cdot \frac{1}{\sqrt{2\pi}\sigma_L} \exp\left(-\frac{(E - E_L)^2}{2\sigma_L^2}\right) + \sum_M I_M \cdot \frac{1}{\sqrt{2\pi}\sigma_M} \exp\left(-\frac{(E - E_M)^2}{2\sigma_M^2}\right), \quad (2)$$

where E_L and E_M are the energies of the L-shell and M-shell X-rays, and I_L and I_M are the corresponding peak intensities. σ_L and σ_M are the energy resolutions at the peak energy. As shown in Fig.1, the K-shell X-ray peaks in the 4~12 keVee spectrum are measured to constrain the intensities of the L/M-shell peaks with known K/L and K/M ratios [11,27]. The energy resolution function $\sigma(E) = a + \sqrt{b \cdot E}$ [28] is fitted by resolutions of K-shell X-ray peaks ($a = 35.5$ eV, $b = 2.8$ eV). Energy resolutions of L/M-shell X-ray peaks are constrained to the $\pm 3\sigma$ uncertainty region of the energy resolution function.

The DM-nucleus interaction cross section is probed by minimizing the χ^2 value at a certain DM mass, and the upper limit at the 90% confidence level (C.L.) is computed using the Feldman-Cousins method [29]. The nuclear recoil quenching factor of Ge calculated by the TRIM software package [11,30–32] with a 10% systematic error is adopted in this analysis like our previous works [26,28].

Fermionic DM Absorption- As proposed in [16,17], the fermionic DM may interact with Ge via a neutral current (NC) absorption, $\chi + Ge \rightarrow \nu + Ge$, modeled as a Yukawa-like interaction with a bosonic mediator. Considering a non-relativistic fermionic DM, its mass dominates its energy and results in a momentum transfer $q \simeq m_\chi$ and nuclear recoil energy $E_R \simeq m_\chi^2/2M$, where M is the mass of the target. The differential event rate (dR_{NC}/dE_R) and total event rate (R_{NC}) of the neutral current absorption signal can be expressed as [17]:

$$\frac{dR_{NC}}{dE_R} = \frac{\rho_\chi}{m_\chi} \cdot \sigma_{NC} \times \frac{1}{M_T} \sum_j N_j M_j A_j^2 F_j^2(m_\chi) \frac{\sqrt{2E_R M_j}}{2p_\nu m_\chi^2} \left\langle \frac{1}{v_\chi} \right\rangle_{v_\chi > v_{min}}, \quad (3)$$

$$R_{NC} = \frac{\rho_\chi}{m_\chi} \cdot \sigma_{NC} \cdot \frac{1}{M_T} \sum_j N_j M_j A_j^2 F_j^2(m_\chi), \quad (4)$$

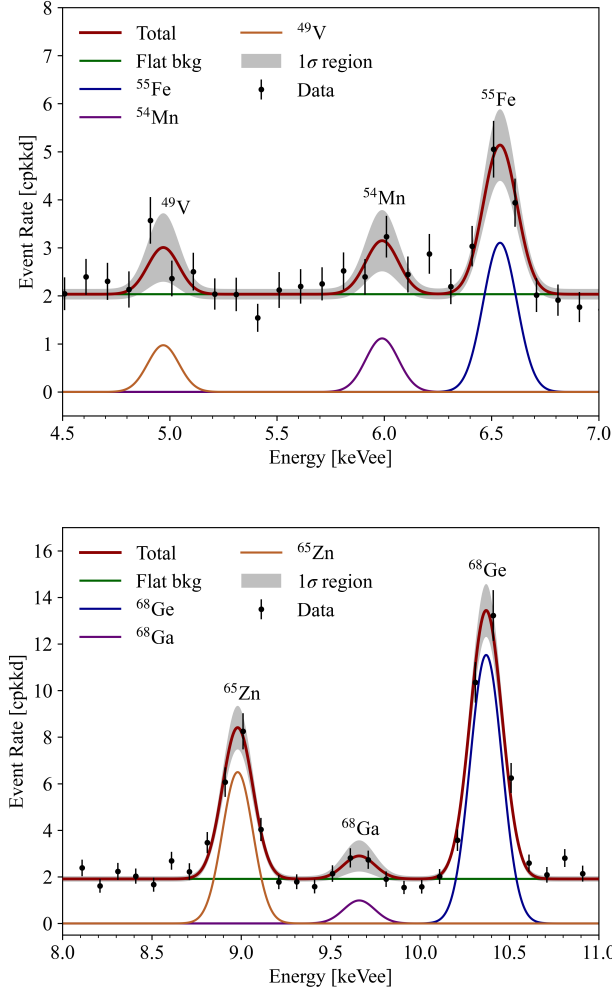


FIG. 1. Spectra fit for the intensities of the six K-shell X-ray peaks, the 1σ uncertainty band derived from the fit uncertainty is labeled in gray. The intensity of L/M-shell X-ray peak is constrained by the K-shell X-ray peak with the known K/L and K/M ratio [11,27].

where σ_{NC} is the DM-nucleon interaction cross section, m_χ is the DM mass. The local DM density ρ_χ is set to 0.3 GeV/cm^3 as recommended in Ref [33]. $M_T = \sum_j N_j M_j$ is the total target mass with N_j and M_j corresponding to the number and mass of isotope j , respectively. $F_j(m_\chi)$ is the normalized Helm form factor for isotope j evaluated at momentum transfer $q = m_\chi$ [34]. $p_\nu = \sqrt{q(2m_\chi - q - 2E_R)}$ denotes the momentum of the outgoing neutrino. v_{min} is the minimum DM velocity at a given recoil energy E_R [17].

As shown in Eq(3), the DM signal rate is contributed by all Ge isotopes, and their abundance in the natural Ge are adopted for the C10-B1 detector: ^{76}Ge (7.6%), ^{74}Ge (36.3%), ^{73}Ge (7.7%), ^{72}Ge (27.5%), and ^{70}Ge (20.9%). Contributions from different Ge isotopes in the nuclear recoil energy spectrum are shown in Fig.2. Converting the nuclear recoil energy in Eq(3) into visible energy and

folding the energy resolution of the detector, the expected spectra of the fermionic DM absorption signals are derived for several m_χ and a certain σ_{NC} , as shown in Fig.3.

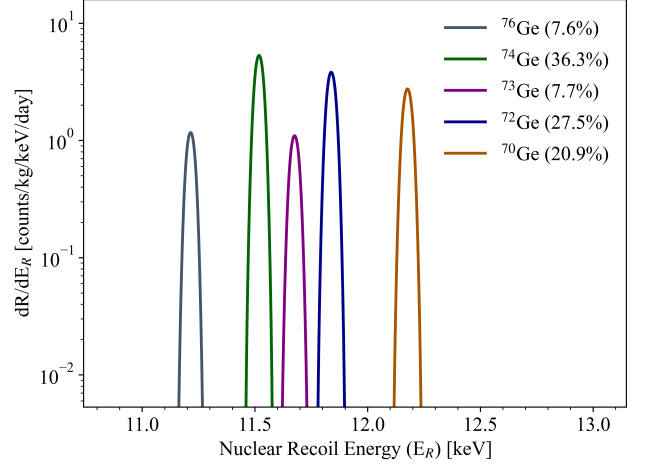


FIG. 2. Nuclear recoil energy spectra of the fermionic DM absorption signals for Ge target, with a DM mass $m_\chi = 40 \text{ MeV/c}^2$ and the DM-nucleon cross section $\sigma_{NC} = 10^{-45} \text{ cm}^2$ for all Ge isotopes.

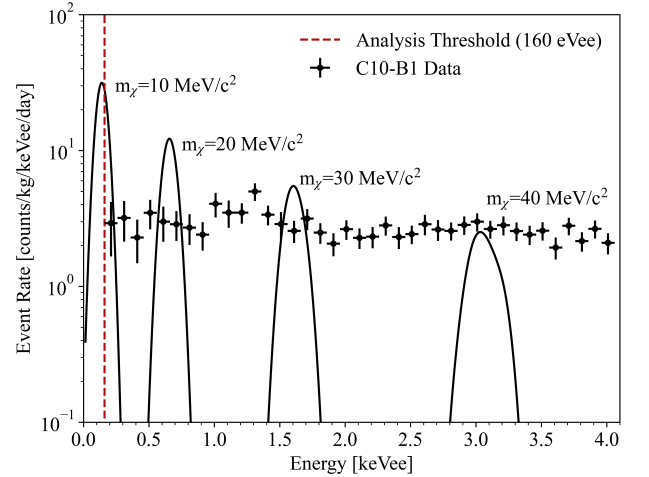


FIG. 3. Expected spectra of the fermionic DM absorption signals for $m_\chi = 10, 20, 30, 40 \text{ MeV/c}^2$ with a DM-nucleon cross section $\sigma_{NC} = 10^{-45} \text{ cm}^2$. The C10-B1 spectrum is shown as the black dots with a bin size of 100 eVee. The red dash line represents the analysis threshold.

We scan the DM mass in the range of $10 \sim 45 \text{ MeV/c}^2$ (corresponding to $0.16 \sim 4 \text{ keVee}$ in the measured energy spectrum), and no significant signal is observed. The best fit spectrum for $m_\chi \sim 40 \text{ MeV/c}^2$ and the corresponding best fit DM peak signature at 3 keVee are displayed in Fig.4. Upper limits of the DM-nucleon cross section superimposed with previous results from direct detection experiments [18,19] and Z_0 monojet searches at the LHC [35] are illustrated in Fig.5. Note that we take

a local DM density (ρ_χ) of 0.3 GeV/cm^3 recommended in [33] other than 0.4 GeV/cm^3 used by the MAJORANA DEMONSTRATOR [19], resulting in more conservative constraints. The most stringent limit on DM-nucleon cross section is $\sigma_{NC} < 2.4 \times 10^{-47} \text{ cm}^2$ at DM mass of $43.0 \text{ MeV}/c^2$ in this work. The upper limit on cross section is set to $\sigma_{NC} < 2.5 \times 10^{-46} \text{ cm}^2$ at $10 \text{ MeV}/c^2$ DM mass.

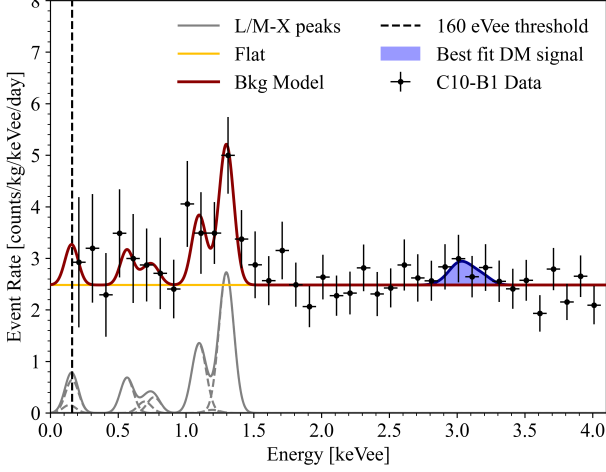


FIG. 4. An example of fermionic DM absorption analysis for $m_\chi = 40 \text{ MeV}/c^2$ with its corresponding best-fit peak signature at 3 keVee . The best-fit background model is shown in the red line, the gray lines represent the contributions from L-shell and M-shell X-ray peaks, and the flat background is depicted by the yellow line. The best-fit DM signal is labeled in blue.

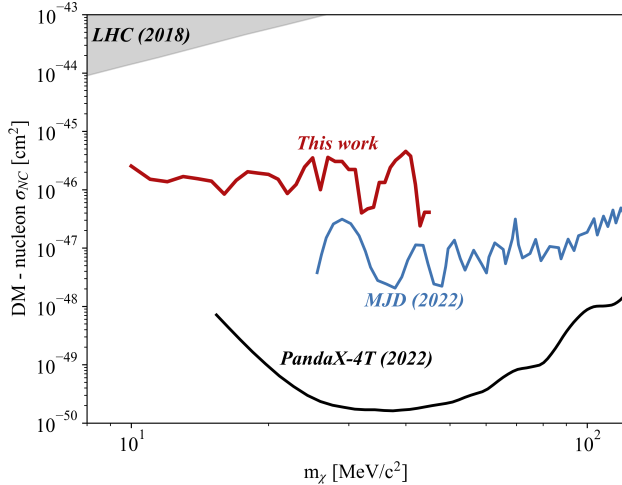


FIG. 5. Upper limit (90% C.L.) of the fermionic DM absorption cross section σ_{NC} . The gray shadow region represents the constraints from Z_0 monojet searches at the LHC (indirect detection). The result from this work is depicted in solid red, results from two other direct detection experiments, the MAJORANA DEMONSTRATOR [19] (MJD, blue line) and PandaX-4T [18] (black line) are superimposed. Constraint on σ_{NC} for DM mass of $>10 \text{ MeV}/c^2$ is achieved in this work.

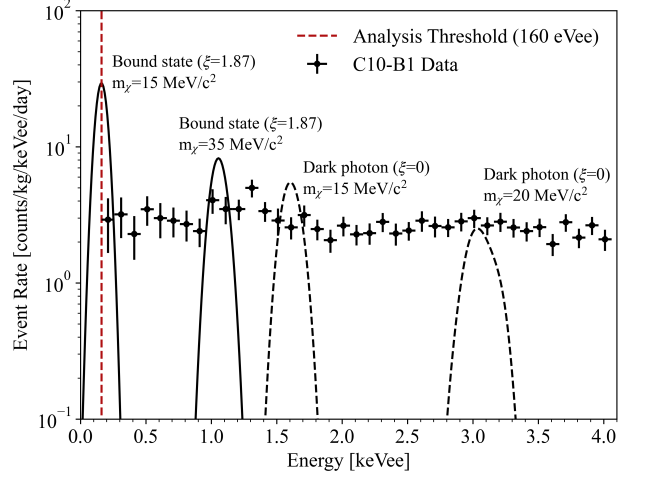


FIG. 6. Expected spectra of the DM-nucleus $3 \rightarrow 2$ scattering signals. Black dashed lines represent the spectra of the massless dark photon final state ($\xi = 0$), black solid lines denote a bound final state ($\xi = 1.87$). The DM-nucleus coupling $\langle \sigma_{3 \rightarrow 2} \cdot v_\chi^2 \rangle n_\chi$ is set to 10^{-45} cm^2 for both final states. The C10-B1 spectrum is shown as the black dots with the red dash line denoting the analysis threshold.

DM-nucleus $3 \rightarrow 2$ scattering- Recent work has proposed that the DM may interact with the nucleus via an inelastic $3 \rightarrow 2$ scattering process, $\chi + \chi + A \rightarrow \phi + A$, where the DM final state (ϕ) can be either a DM composite state or any dark radiation [21]. The signature of this process is similar to that of the fermionic DM absorption. Neglecting the initial kinetic energy of the DM particles, the monoenergetic nuclear recoil energy is:

$$E_R \simeq \frac{(4 - \xi^2)m_\chi^2}{2(M + 2m_\chi)}, \quad (5)$$

where M is the mass of the nucleus, ξ is the mass ratio of the final and initial dark matter states ϕ and χ . The mass ratio ξ is model-dependent. In this study, we considered two models: a massless DM final state ($\phi = \text{dark photon}$, $\xi = 0$) and a bound DM final state. For the bound DM final state, the mass ratio $\xi = 2(m_\chi + \epsilon)/m_\chi$, where the binding energy ϵ is decided by a new gauge coupling g_D : $\epsilon = -(g_D^4 \cdot m_\chi)/(64\pi^2)$ [36]. We set the gauge coupling $|g_D| = 3$ as in [21] and obtain a mass ratio $\xi = 1.87$ for the bound DM final state.

The total event rate of the $3 \rightarrow 2$ scattering is similar in form to that of the fermionic DM absorption:

$$R_{3 \rightarrow 2} = \frac{\rho_\chi}{m_\chi} \cdot n_\chi \langle \sigma_{3 \rightarrow 2} \cdot v_\chi^2 \rangle \times \frac{1}{M_T} \sum_j N_j M_j A_j^2 F_j^2(q_{3 \rightarrow 2}), \quad (6)$$

where the $\langle \sigma_{3 \rightarrow 2} \cdot v_\chi^2 \rangle$ is the average three-body inelastic cross section with a DM initial velocity of v_χ . $n_\chi =$

ρ_χ/m_χ is the number density. The momentum transfer in the $3 \rightarrow 2$ scattering is $q_{3 \rightarrow 2} = \sqrt{4 - \xi^2} m_\chi$. In the calculation of DM expected spectra, the quenching factor and energy resolution are the same as in fermionic DM absorption calculation. Fig.6 shows the expected spectra of the $3 \rightarrow 2$ scattering signals for the massless dark photon and bound DM final state. The shape of the expected spectra is also similar to that of the fermionic DM absorption.

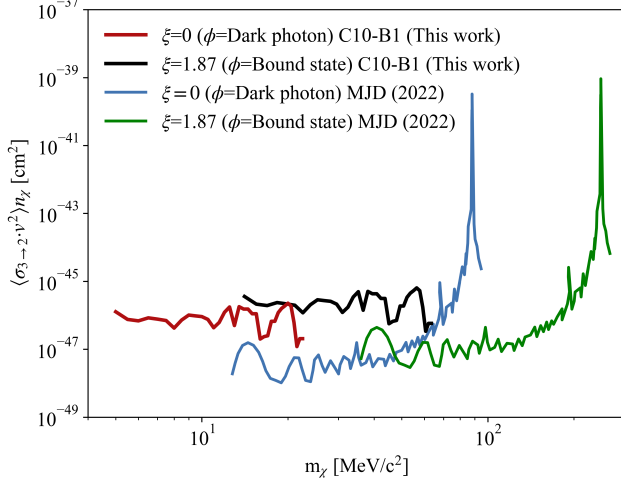


FIG. 7. Upper limit (90% C.L.) of the DM-nucleus $3 \rightarrow 2$ scattering coupling $\langle \sigma_{3 \rightarrow 2} \cdot v_\chi^2 \rangle n_\chi$. $\xi = 0$ is a massless dark photon final state, and $\xi = 1.87$ is a bound state. The results of this work (red and black lines) are compared with the results from the MAJORANA DEMONSTRATOR (MJD, blue and green lines). The MJD takes a local DM density (ρ_χ) of 0.4 GeV/cm^3 [19], while this work takes a ρ_χ of 0.3 GeV/cm^3 as recommended in [33]. This work places limits on a lower DM mass region for both massless and bound DM final states with a lower analysis threshold of 160 eVee.

We place limits on the $(m_\chi, \langle \sigma_{3 \rightarrow 2} \cdot v_\chi^2 \rangle n_\chi)$ parameter

as suggested in Ref [21] for the massless dark photon and the bound DM final state. The 90% upper limit for the coupling $\langle \sigma_{3 \rightarrow 2} \cdot v_\chi^2 \rangle n_\chi$ is shown in Fig.7. Compared with the results from the MAJORANA DEMONSTRATOR [19], this work achieved a lower analysis threshold of 160 eVee and excluded new parameter space in lower DM mass regions.

Conclusion- In this Letter, we report search results for the sub-GeV fermionic DM absorption and DM-nucleus $3 \rightarrow 2$ scattering using 205.4 kg·day exposure data from the C10-B1 PPCGe detector in the CDEX-10 experiment. The expected DM signal is analyzed in the 160 eVee~4 keVee spectrum via a minimum χ^2 method. With an analysis threshold of 160 eVee, we set new experimental limits on the fermionic DM absorption cross section in $10 \sim 45 \text{ MeV/c}^2$ DM mass. For the DM-nucleus $3 \rightarrow 2$ scattering, we place limit on lower DM mass of 5 MeV/c^2 for a massless dark photon DM final state, and 14 MeV/c^2 for the bound DM final state. Those limits achieve the lowest DM mass among the searches in direct detection experiments to date.

ACKNOWLEDGMENTS

This work was supported by the National Key Research and Development Program of China (Grant No. 2017YFA0402200) and the National Natural Science Foundation of China (Grants No. 12175112, No. 12005111, No. 11725522, No. 11675088, No.11475099). We would like to thank CJPL and its staff for hosting and supporting the CDEX project. CJPL is jointly operated by Tsinghua University and Yalong River Hydropower Development Company.

-
- [1] B. L. Young, *Front. Phys.* **12**, 121201 (2017).
 - [2] J. Liu, *et al.* *Nature Phys.* **13**, 212 (2017),
 - [3] C. Patrignani, *et al.* *Chin. Phys. C* **40**, 100001 (2016).
 - [4] J. Billard, *et al.* *Rep. Prog. Phys.* **85**, 056201 (2022).
 - [5] D. S. Akerib, *et al.* (LUX Collaboration), *Phys. Rev. Lett.* **118**, 021303 (2017)
 - [6] Y. Meng *et al.* (PandaX Collaboration), *Phys. Rev. Lett.* **127**, 261802 (2021).
 - [7] E. Aprile *et al.* (XENON Collaboration) *Phys. Rev. Lett.* **121**, 111302 (2018).
 - [8] P. Agnes *et al.* (DarkSide Collaboration), *Phys. Rev. D* **98**, 102006 (2018).
 - [9] R. Agnese, *et al.* (SuperCDMS Collaboration), *Phys. Rev. D* **99**, (2019).
 - [10] G. Angloher, *et al.* (CRESST Collaboration), *Eur. Phys. J. C* **76**, 25 (2016).
 - [11] H. Jiang *et al.* (CDEX Collaboration) *Phys. Rev. Lett.* **120**, 241301 (2018).
 - [12] L. T. Yang *et al.* (CDEX Collaboration) *Chin. Phys. C* **42**, 023002 (2018).
 - [13] A. Kusenko, *Phys. Rep.* **481**, 1 (2009).
 - [14] M. Pospelov, *et al.* *Phys. Rev. D* **78**, 115012 (2008).
 - [15] K. Rajagopal, *et al.* *Nucl. Phys. B* **358**, 447 (1991).
 - [16] J. A. Dror, *et al.* *Phys. Rev. Lett.* **124**, 181301 (2020).
 - [17] J. A. Dror, *et al.* *J. High Energy Phys.* **2020**, (2019).
 - [18] L. Gu, *et al.* (PandaX Collaboration), *Phys. Rev. Lett.* **129**, 161803 (2022).
 - [19] I.J. Arnquist, *et al.* (Majorana Collaboration), *arXiv:2206.10638*, (2022).
 - [20] T. Li, J. Liao, and R.-J. Zhang, *J. High Energy Phys.* **05**, 071. (2022).
 - [21] W. Chao, *et al.* *arXiv:2109.14944*. (2021).

- [22] J. P. Cheng, *et al.* Annu. Rev. Nucl. Part. Sci. **67**, 231 (2017).
- [23] H. Jiang, *et al.* (CDEX Collaboration), Sci. China-Phys.Mech. Astron. **62**, 31012 (2019).
- [24] Z. She, *et al.* (CDEX Collaboration), Phys. Rev. Lett. **124**, 111301 (2020)
- [25] L. T. Yang, *et al.* Nucl. Instrum. Methods Phys. Res., Sect A **886**, 13 (2018).
- [26] Q. Yue, *et al.* (CDEX Collaboration), Phys. Rev. D **90**, 091701 (2014).
- [27] J. N. Bahcall, Phys. Rev. **132**, 362 (1963).
- [28] W. Zhao, *et al.* (CDEX Collaboration), Phys. Rev. D **93**, 092003, (2016).
- [29] G. J. Feldman and R. D. Cousins, Phys. Rev. D **57**, 3873 (1998).
- [30] A.K. Soma, *et al.* Nucl. Instrum. Methods A **836**, 67 (2016).
- [31] B. J. Scholz, *et al.* Phys. Rev. D **94**, 122003 (2016).
- [32] J. F. Ziegler, Nucl. Instrum. Methods B **1027**, 219–220 (2004).
- [33] D. Baxter, *et al.* Eur. Phys. J. C **81**, 907 (2021).
- [34] J. D. Lewin and P. F. Smith, Astropart. Phys. **6**, 87 (1996).
- [35] A. Belyaev, *et al.* Phys. Rev. D **99**, 015006 (2019).
- [36] K. Petraki, *et al.* J. High Energy Phys. **2015**, 1 (2015).